



# Study of Plasma- and Detonation Gun-Sprayed Alumina Coatings Using Taguchi Experimental Design

P. Saravanan, V. Selvarajan, M.P. Srivastava, D.S. Rao, S.V. Joshi, and G. Sundararajan

(Submitted 5 May 1999)

Atmospheric plasma spraying (APS) is a most versatile thermal spray method for depositing alumina ( $\text{Al}_2\text{O}_3$ ) coatings, and detonation gun (D-gun) spraying is an alternative thermal spray technology for depositing such coatings with extremely good wear characteristics. The present study is aimed at comparing the characteristics of  $\text{Al}_2\text{O}_3$  coatings deposited using the above techniques by using Taguchi experimental design.

Alumina coating experiments were conducted using a Taguchi fractional-factorial ( $L_8$ ) design parametric study to optimize the spray process parameters for both APS and D-gun. The Taguchi design evaluated the effect of four APS and D-gun spray variables on the measured coating attributes. The coating qualities evaluated were surface roughness, porosity, microhardness, abrasion, and sliding wear. The results show that the coating quality is directly related to the corresponding coating microstructure, which is significantly influenced by the spray parameters employed. Though it is evident that the D-gun-sprayed coatings consistently exhibit dense and uniform microstructure, higher hardness, and superior tribological performance, the attainment of suitable plasma-sprayed coatings can be improved by employing the Taguchi analysis.

**Keywords** abrasion, alumina coating, design of experiments, d-gun coatings, DOE, optimization, plasma spray coatings, sliding wear, Taguchi analysis

## 1. Introduction

The application areas of plasma-sprayed alumina ( $\text{Al}_2\text{O}_3$ ) coatings have grown, particularly in the field of combating wear.<sup>[1-4]</sup> Although it is widely recognized that APS of  $\text{Al}_2\text{O}_3$  coatings can provide solutions to engineering problems, its ability to satisfy the requirements where high wear resistance is of great importance has to be raised. On the other hand, D-gun spraying is another promising thermal spray technology for depositing such coatings with extremely good wear characteristics.<sup>[5,6,7]</sup> However, the literature reveals that there have been very few studies ascertaining the relative performance of plasma- and D-gun-sprayed coatings.<sup>[6,7,8]</sup>

Exploitation of any coating system will lie in the generation and acceptance of appropriate quality assurance, *i.e.*, a repeatable achievement of high-quality coatings. Hence, it is necessary to characterize, fully understand, and interpret the performance of such coatings. For most thermal spray processes, the optimization of the spray parameters is not a trivial task. This is primarily due to the large number of processing parameters or factors involved. Design of experiments (DOE) is an effective

method for conducting experiments to enhance thermal spray coating properties through producing optimum values of spray parameters. A DOE only leads to correlations, not physical understanding.

Taguchi-type fractional-factorial designs are an efficient means of determining the effects of process parameters on the measured responses. They are easy to plan and readily adaptable to both continuous factors (*i.e.*, those which are controllable at preset values) and discrete factors (*i.e.*, those which are orderable but not measurable). Major advantages of using Taguchi methods include the ability to separate the effect of various factors that may have similar behavior and the ability to determine the effect of a factor whose magnitude may have the same order of magnitude as the error terms. Recently, plasma and high velocity oxy-fuel spray parameters have been successfully optimized using DOE techniques,<sup>[9-12]</sup> particularly the Taguchi method, but no such optimization studies have been carried out for the D-gun spray process.

## 2. Experimental Details

### 2.1 Description of the Taguchi Method

A Taguchi-style<sup>[13,14]</sup> design of experiment, *i.e.*,  $L_8$  ( $2^{4-1}$ )-eight run, fractional-factorial, studying four process parameters, each at two levels, was employed to study the effect of selected process parameters on the quantitatively measured coating attributes. Prior experience helped the authors to identify the major process parameters and their operational ranges in the APS and D-gun spray process. Care was taken to avoid overwhelming the matrix by one parameter being unusually broader than the others. The main process parameters selected for the APS processes were primary gas flow, plasma arc current, powder feed rate, and

P. Saravanan and V. Selvarajan, Department of Physics, Bharathiar University, Coimbatore 641 046, India; M.P. Srivastava, Defence Metallurgical Research Laboratory, Hyderabad 500 058, India; and D.S. Rao, S.V. Joshi, and G. Sundararajan, International Advanced Research Centre for Powder Metallurgy & New Materials, Hyderabad 500 005, India. Contact e-mail: physics@250.bharathi.ernet.in.

**Table 1** Design of experiment with main variables for APS

Process parameter/factor	Levels		
	Lower (-1)	Standard (0)	Higher (+1)
Primary gas flow, L/min	64	71	78
Plasma arc current, A	450	500	550
Powder feed rate, g/min	20	25	30
Spray distance, mm	60	75	90

**Table 2** Design of experiment with main variables for D-gun

Process parameter/factor	Levels		
	Lower (-1)	Standard (0)	Higher (+1)
Fuel ratio (C <sub>2</sub> H <sub>2</sub> /O <sub>2</sub> )	1:2.8	1:2.4	1:2.0
Carrier gas flow rate, L/s	1.33	2.27	3.21
Frequency of detonations, Hz	2	3	4
Spray distance, mm	180	200	220

spray distance. In the case of the D-gun process, fuel ratio, *i.e.*, acetylene to oxygen ratio (C<sub>2</sub>H<sub>2</sub>/O<sub>2</sub>), carrier gas flow rate, frequency of detonations, and spray distance were the main process parameters. Each parameter has two levels, selected to vary around the standard settings. The natural and coded values of the main variables are given in Tables 1 and 2 for the APS and D-gun processes, respectively. Coating experiments PA01 through PA09 and DA01 through DA09 representing the eight runs evaluated (including the standard settings) with the Taguchi (L<sub>8</sub>) approach are shown in Tables 3 and 4 for APS and D-gun spray processes, respectively. The experimental runs of a given design were performed in a random order to reduce the influence of potential systematic errors.

After the experiments were conducted per the designed factors, the data were obtained for the coating attributes, *viz.*, surface roughness, porosity, microhardness, abrasion, and sliding wear. The experimental data was subjected to multiple regression analysis and analysis of variance (ANOVA) for each specific coating attribute to select the significant level of the process parameter and to understand the magnitude of influence that each variable had on the coating properties. From the ANOVA calculations, *rho* percent contribution or *rho* percent ( $\rho\%$ ) was calculated. The  $\rho$  value indicates the influence of the process parameter on the measured coating attribute, with a larger value indicating stronger influence. The description of statistical terms used in this study, as well as their analyses, is found in Ref 13 to 15. The Taguchi analysis was accomplished with GWBASIC programs.

## 2.2 Substrate and Coating Materials

Mild steel (0.25% C, 0.7% Mn, 0.25% Si, and 0.05% S) substrates were employed throughout for coating deposition. Samples with the following dimensions were used to prepare coated specimens for different wear tests.

- Abrasion wear: 75 × 25 × 15 mm.
- Sliding wear: pin—6 mm diameter, 30 mm length.

**Table 3** Taguchi experimental design test matrix (L<sub>8</sub>) for plasma spraying of alumina coatings

Run number	Primary gas flow, L/min	Plasma arc current, A	Powder feed rate, g/min	Spray distance, mm
PA01	78/+1	550/+1	30/+1	90/+1
PA02	78/+1	550/+1	20/-1	60/-1
PA03	78/+1	450/-1	30/+1	60/-1
PA04	78/+1	450/-1	20/-1	90/+1
PA05	64/-1	550/+1	30/+1	60/-1
PA06	64/-1	550/+1	20/-1	90/+1
PA07	64/-1	450/-1	30/+1	90/+1
PA08	64/-1	450/-1	20/-1	60/-1
PA09	71/0	500/0	25/0	75/0

**Table 4** Taguchi experimental design test matrix (L<sub>8</sub>) for detonation spraying of alumina coatings

Run number	Fuel ratio (C <sub>2</sub> H <sub>2</sub> /O <sub>2</sub> )	Carrier gas flow rate, L/m	Frequency of detonations, Hz	Spray distance, mm
DA01	1:2.0/+1	3.21/+1	4/+1	220/+1
DA02	1:2.0/+1	3.21/+1	2/-1	180/-1
DA03	1:2.0/+1	1.33/-1	4/+1	180/-1
DA04	1:2.0/+1	1.33/-1	2/-1	220/+1
DA05	1:2.8/-1	3.21/+1	4/+1	180/-1
DA06	1:2.8/-1	3.21/+1	2/-1	220/+1
DA07	1:2.8/-1	1.33/-1	4/+1	220/+1
DA08	1:2.8/-1	1.33/-1	2/-1	180/-1
DA09	1:2.4/0	2.27/0	3/0	200/0

- In the case of the sliding wear tests, the coated pin was tested against WC-12%Co D-gun coated discs, since it has comparatively higher hardness and wear resistance than the alumina coating.<sup>[16]</sup> Commercially available thermal spray powder (Metco 105 SF alumina) used for coating deposition was procured from Sulzer-Metco. The powder ranged in size from +5 to 20  $\mu\text{m}$ .

## 2.3 Precoating Substrate Preparation

Prior to coating by both APS and D-gun processes, the substrates were roughened by air blasting using alumina grit of -60 mesh. The blasting was performed at an air pressure of approximately 0.5 MPa. Subsequent to grit blasting, the samples were ultrasonically cleaned.

## 2.4 Powder Characterization

Particle size analysis of the spray-grade powder was performed (illustrated in Table 5) using a laser particle size analyzer CILAS 920 (Cilas Le Sens de la Mesure, Marcoussias, France). The powder particle size determined from the analysis generally conforms to the data given by the manufacturer. Scanning electron microscopy (SEM) was used to observe the morphology of the powder.

## 2.5 Deposition of Alumina Coatings

Plasma spray deposition of Al<sub>2</sub>O<sub>3</sub> powder was performed using a Metco 7MB APS unit. The spray parameters employed

**Table 5** Characterization of alumina powder

Powder	Manufacturer	Chemical composition, wt %	Particle size, $\mu\text{m}$			Particle shape
			Diam at 10%	Diam at 90%	Mean value	
$\text{Al}_2\text{O}_3$	Sulzer-Metco	$\text{Al}_2\text{O}_3$ - (bal) $\text{SiO}_2$ - 0.0015 $\text{Fe}_2\text{O}_3$ - 0.0190 $\text{Cr}_2\text{O}_3$ - 0.0016 $\text{TiO}_2$ - 0.0033	2.06	10.95	16.26	Regular and angular blocky

**Table 6** Plasma spray parameters for spraying of alumina powder

Primary gas (Ar)	
Pressure, MPa	0.69
Flow, L/min	64–78
Secondary gas ( $\text{H}_2$ )	
Pressure, MPa	0.35
Flow, L/min	4.70
Carrier gas (Ar)	
Flow, L/min	28.3
Powder feed rate, g/min	20–30
Plasma arc current, A	450–550
Spray distance, mm	63–89

**Table 7** Main characteristics of D-gun spray equipment

Barrel length, mm	1800
Barrel diameter, mm	22
Working gases:	
Fuel	Acetylene
Oxidizer	Oxygen
Powder carrier gas	Nitrogen
Firing frequency, Hz	2–4
Coating thickness per cycle, $\mu\text{m}$	5–20
Typical coating thickness	50–500
Power consumption per hour, kW	2

for depositing the  $\text{Al}_2\text{O}_3$  powder under investigation are listed in Table 6. The D-gun unit used was of Ukrainian origin. A combustible gas mixture consisting of oxygen and acetylene was periodically detonated using a spark plug. The D-gun parameters employed for coating deposition are listed in Table 7. Further details regarding the D-gun spray equipment and its characteristics have been reported elsewhere.<sup>[17]</sup> Care was taken to ensure that the coating thickness was approximately the same and was in the range of  $215 \pm 30 \mu\text{m}$  for both plasma and D-gun spraying to facilitate comparison.

## 2.6 Characterization of Coatings

The microstructural features of the coated specimens were studied using standard metallographic techniques. A sample was cut, mounted, and polished and its cross section observed under an optical microscope for all the runs of the deposited coatings. The porosity of the coatings was measured using a metallurgical microscope fitted with an image analyzer (Quantimet Q-520). An optical microscope was used to study the surface morphology of as-sprayed coatings. Vickers microhardness values were obtained on the cross-sectioned surface of the coating using a microhardness tester under 0.2 kg load. The thickness of the

**Table 8** Abrasive wear test conditions

Abrasive material	Silica (150–250 $\mu\text{m}$ )
Rotation speed of the wheel, rev/min	200
Load used, N	50
Duration of the test, s	60
Sand feed rate, g/min	200

**Table 9** Sliding wear test conditions

Disk speed, rev/min	820
Sliding velocity, m/s	3.20
Track radius, mm	36
Sliding distance, km	5.50
Load applied, N	20
Duration of test, min	30
Relative humidity, %	$55 \pm 3$
Test temperature, $^{\circ}\text{C}$	25

coatings was measured by using an eddy current coating thickness gage and by using an optical microscope. The surface roughness,  $R_a$ , of the coatings was also determined.

## 2.7 Wear Tests

**2.7.1 Abrasion Wear Test.** To evaluate the abrasive wear resistance property of the plasma-sprayed and D-gun-coated samples, a dry sand-rubber wheel abrasion test rig was used. Testing was performed in accordance with ASTM G-65<sup>[18]</sup> and the conditions used are given in Table 8. The specimens were cleaned ultrasonically with acetone and weighed before and after the tests. From the results of the abrasive wear loss, the relative abrasion wear resistance (RAWR) values of all the alumina coatings were calculated. In this figure, RAWR is defined as the ratio of abrasive wear loss suffered by the bare mild steel specimen to the abrasive wear loss suffered by the coated mild steel specimen under identical abrasion test conditions.<sup>[19]</sup>

**2.7.2 Sliding Wear Test.** The sliding wear tests were performed using a pin-on-disk tribometer employing the conditions listed in Table 9. Both the pin and coated disk samples were ultrasonically cleaned in acetone separately and before and after the test. The weight loss due to sliding wear of the pin was calculated. The wear rate was calculated from the volume loss (in cubic millimeters) divided by the normal load (in Newtons) and sliding distance (in meters). The volume loss was obtained from the mass loss divided by the coating density. In the present study, the coating density of  $\text{Al}_2\text{O}_3$  ( $3.4 \text{ g/cm}^3$ ) reported elsewhere<sup>[20]</sup> was assumed for converting mass loss into volume loss.

**Table 10** Coating characterization results for plasma spraying

Number L8 Run	Thickness, $\mu\text{m}$	Roughness $R_a$ , $\mu\text{m}$	Hardness, Hv	Porosity, %	Relative abrasive wear resistance	Wear rate, $\times 10^{-6}$ $\text{mm}^3/\text{N m}$
PA01	185	3.34-O	884	8.18	37.15	4.635-L
PA02	198	3.80	1043-O	3.75-O	128.59-O	2.276
PA03	195	3.92	996	7.83	94.99	2.234
PA04	220	3.66	803	9.81	47.10	4.301
PA05	206	3.94-L	989	4.50	188.84	1.357-O
PA06	188	3.51	774	9.97	20.04	1.611
PA07	196	3.69	696-L	16.22-L	14.28-L	1.670
PA08	200	3.88	987	6.64	113.10	3.862
PA09	210	3.48	936	5.61	102.58	1.733
NM	10	10	10	10	...	...
Error, %	$\pm 7$	$\pm 5.2$	$\pm 4$	$\pm 6.6$	...	...

NM: number of measurements performed for each test  
L denotes the lowest value and O the optimum value in the experimental matrix

**Table 11** Coating characterization results for D-gun

Number L8 Run	Thickness, $\mu\text{m}$	Roughness $R_a$ , $\mu\text{m}$	Hardness, Hv	Porosity, %	Relative abrasive wear resistance	Wear rate, $\times 10^{-6}$ $\text{mm}^3/\text{N m}$
DA01	214	4.61	957	7.20	92.07	3.132-L
DA02	195	9.14-L	1183	1.46	199	1.273
DA03	221	8	1257-O	1.07-O	234.64-O	2.171
DA04	229	3.79-O	1072	4.30	145.23	0.438-O
DA05	212	8.92	1027	5.28	154.50	2.881
DA06	244	5.88	997	9.91	87.58	1.189
DA07	195	6.32	935-L	10.23-L	58.82-L	2.312
DA08	209	9.52	1054	6.77	108.60	2.422
DA09	220	5.90	1110	2.41	173.95	0.167
NM	10	10	10	10	...	...
Error, %	$\pm 8$	$\pm 6$	$\pm 3$	$\pm 5$	...	...

NM: number of measurements performed for each test  
L denotes the lowest value and O the optimum value in the experimental matrix

### 3. Results and Discussion

The summaries of the coating characterization results for the experiments are presented in Tables 10 and 11 for the plasma and D-gun-sprayed  $\text{Al}_2\text{O}_3$  coatings.

#### 3.1 Surface Roughness

The coating  $R_a$  values ranged from 3.34 to 3.94  $\mu\text{m}$  for the APS coatings, which indicates that the variations in plasma processing conditions moderately affect the surface roughness. However, the size distribution of the powder may influence the surface roughness. From the ANOVA calculations, it was confirmed that the spray distance was the most dominant factor in reducing the surface roughness; it has a contribution ratio of 71.6% at the higher level in lowering the roughness.

For the D-gun coatings, the  $R_a$  values ranged from 3.79 to 9.14  $\mu\text{m}$ . The higher variation in the roughness of the D-gun coatings may be attributed either to the higher percentage of variation ( $\pm 10$ ) selected for spray distance or to the possible significantly wider distribution of velocities of particles in D-gun spraying. Though the variation in the surface roughness range is higher than that of the APS coatings, spray distance alone had a dominant influence (84.1%) on the surface roughness similar to

that of the APS coatings. Other parameters have only smaller contribution ratios in lowering the roughness for both plasma and D-gun spraying.

#### 3.2 Porosity Exhibited

From the image analysis of metallographically prepared surfaces, porosity was determined as listed in Tables 10 and 11 for the APS and D-gun coatings. Ten fields were selected for the measurement of porosity (each field covered by 1.19  $\text{mm}^2$  area) and the average porosity values of the alumina coatings ranged from 3.75 to 16.22% for APS coatings. Coating PA02 exhibited the lowest porosity, whereas coating PA07 had the highest porosity in the APS experimental matrix. From the ANOVA calculations, it was confirmed that the parameters' spray distance (54.4%) at lower level and plasma arc current (23.5%) at higher level are significant in lowering the porosity. Other contributors were primary gas flow at 7.1%, with the higher primary gas flow resulting in lower porosity, and powder feed rate at 5%, with the lower feed rate resulting in lower porosity. For a given coating material, the porosity is related to the particle size distribution of the powder and to the temperature and velocity of the particles on impact. Clearly, the lowest-porosity coatings would be expected for a stream of completely molten particles with high ve-

locity.<sup>[21]</sup> In general, higher arc current produces high heat input to the particles and higher primary gas flows produce higher flame velocities, resulting in particles predicted to be in a highly molten state and attaining higher velocities before impinging on the substrate. Hence, in the present study, lower porosity had been achieved at the higher levels of primary gas flow and arc current and lower levels of spray distance.

The average porosity values ranged from 1.07 to 10.23% for D-gun coatings. Coating DA03 revealed the lowest porosity, whereas coating DA07 had the highest porosity in the D-gun experimental matrix. Spray distance (45.9%) and fuel ratio (30.4%) were the two dominant factors affecting the porosity. Porosity decreases with increase in fuel ratio and decrease in spraying distance. Other parameters have only smaller contribution ratios in lowering the roughness for the D-gun spraying. Generally, it is considered that a sufficiently high particle velocity will lead to the production of a dense coating with low porosity. At higher fuel ratio and shorter spray distances, particles are well molten and impinge with high velocities on the substrate and, hence, result in lower porosity at such conditions.

### 3.3 Microstructure of the As-Sprayed $Al_2O_3$ Coatings

The microstructures of all the coatings were studied by optical microscopy and SEM. All the coatings produced in the experimental matrix may be graded from poor to excellent in quality. Figure 1(a) to (c) depict the typical microstructures of as-deposited APS coatings for the experimental runs: PA02 (lowest porosity and highest hardness), PA07 (highest porosity and poor hardness), and P09 (coating generated from standard parameters). Coatings deposited at lower arc current and shorter spray distances exhibited a significant amount of unmelted particles and a macroporosity. In the present study, it is quite understandable that at higher primary gas flows, higher arc currents, and shorter spray distances, the particles are at good molten state and impinge with higher velocities on the substrate. Hence, dense and uniform microstructures are obtained under such conditions.

Figure 2(a) to (c) depict the typical microstructures of as-deposited D-gun coatings for the experimental runs: DA03 (lowest porosity and highest hardness), DA07 (highest porosity and poor hardness), and DA09 (coating generated from standard parameters). All the photomicrographs exhibited very dense coatings with homogeneously dispersed microporosity; no cracking or large amounts of unmelted particles were observed except for sample DA07. A comparison of the as-sprayed microstructures of the APS and D-gun coated  $Al_2O_3$  coatings reveals that the APS coating is less dense relative to the D-gun coating. These findings can be attributed to the significantly higher particle velocities that are obtained in D-gun spraying.<sup>[22,23,24]</sup>

### 3.4 Microhardness Measurements

The average microhardness values measured in all the  $Al_2O_3$  coatings for both the APS and D-gun processes are given in Tables 10 and 11. For the APS process, the hardness values ranged from 696 to 1043 Hv. Coating PA02 exhibited the highest hardness, whereas coating PA07 had the lowest hardness in the experimental matrix. For higher hardness, spray distance alone was

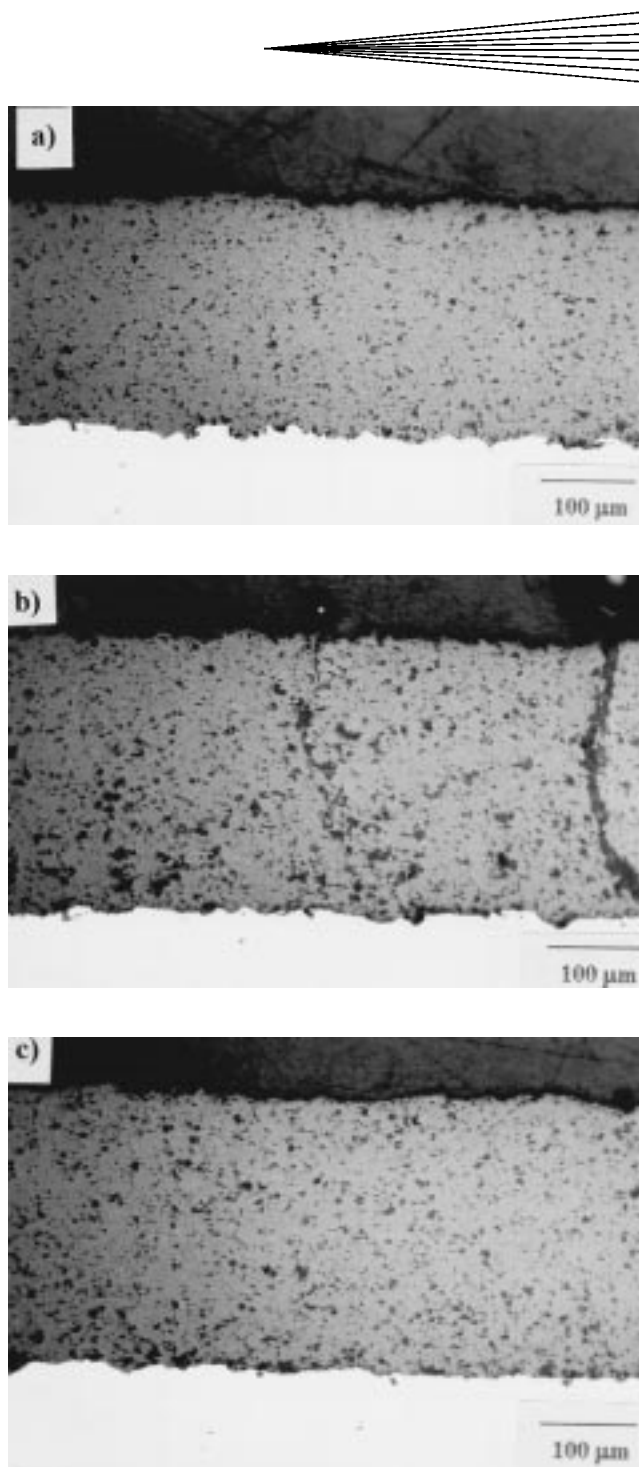


**Fig. 1.** Optical micrographs of as-sprayed  $Al_2O_3$  coatings deposited by APS. (a) PA02, coating of good quality; (b) PA07, coating of poor quality; and (c) PA09, coating generated from standard parameters (200 $\times$ )

found to be significant and it has a contribution ratio of 82%. Other contributors were primary gas flow (8.73%) and plasma arc current (4.82%) in increasing the hardness. In general, good adherence and higher hardness are expected when the particles are molten and strike the surface, they have sufficient momentum to assure intense contact upon impact, and the contact temperature is as high as possible. At higher primary gas flows and arc currents and shorter spray distances, the particles are pre-

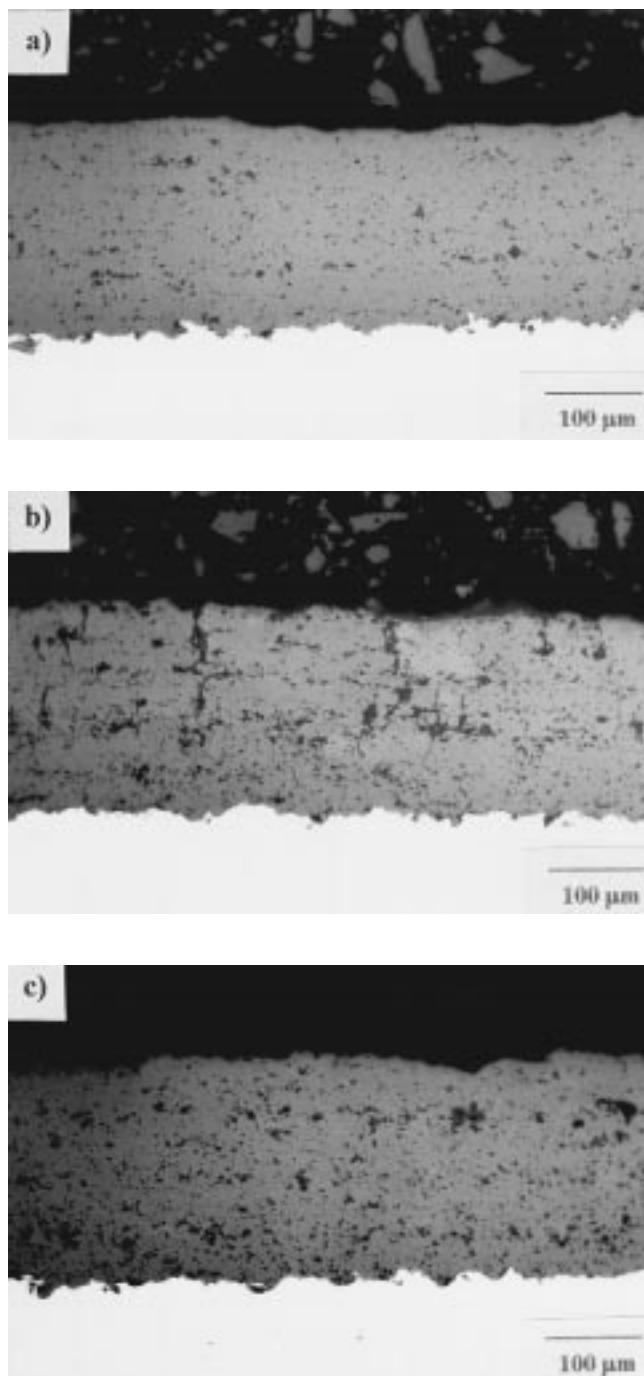


**Fig. 2.** Optical micrographs of as-sprayed  $\text{Al}_2\text{O}_3$  coatings deposited by D-gun. (a) DA03, coating of good quality; (b) DA07, coating of poor quality; and (c) DA09, coating generated from standard parameters (200 $\times$ )

dicted to be in a highly molten state and to attain higher velocities before impinging the substrate. Hence, in the present study, higher hardness had been achieved at the higher levels of primary gas flow and arc current and lower levels of spray distance in the APS process.

For the D-gun process, the hardness values ranged from 935 to 1257 Hv. Coating DA03 had the highest hardness, whereas

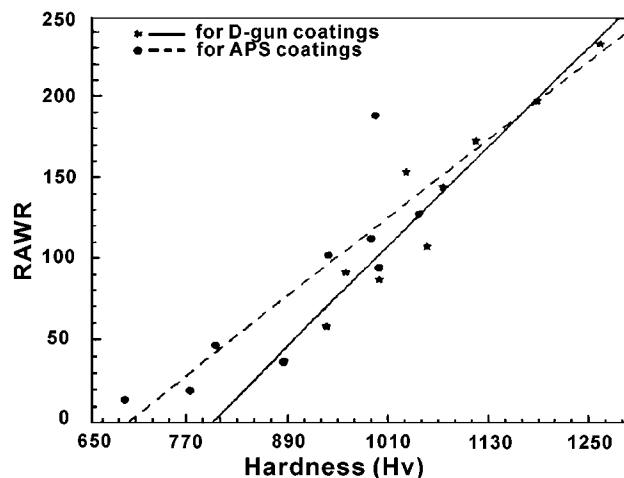


**Fig. 3.** Correlation between hardness and RAWR of the  $\text{Al}_2\text{O}_3$  coatings deposited by APS (dashed line) and D-gun (solid line)

coating DA07 had the lowest hardness. Spray distance (45.9%) and fuel ratio (30.4%) were the two contributing factors affecting the hardness. The hardness of D-gun coatings is consistently higher than that of APS coatings; this finding is consistent with the trends reported in other studies comparing plasma and D-gun-sprayed coatings.<sup>[7,8]</sup> This finding also may be partly attributed to previously noted superior microstructures resulting from the D-gun process. In general, at a higher fuel ratio and a shorter spray distance, particles attain higher velocities and so more accelerating particles adhere to the coating matrix and hence a higher hardness is obtained.

### 3.5 Wear Test Results

**3.5.1 Abrasion Test Results.** All the APS and D-gun coatings studied were subjected to abrasion wear tests. The wear resistance in all the D-gun coatings was much higher than that obtained with the APS coatings. The calculated RAWR values ranged from 128.59 to 14.28 for the APS process, whereas these values ranged from 234.64 to 58.82 for the corresponding D-gun coatings. Coatings with higher RAWR are more abrasive wear resistant. For abrasive wear resistance, the spray distance was the most dominating factor for both the APS and D-gun processes, and primary gas flow and fuel ratio were the second significant factors for the APS and D-gun, respectively. The variation in the RAWR for all the coatings indicates that all the APS coatings exhibit a consistently higher wear rate than the corresponding D-gun coatings, which show significantly lower wear. From both the coating characterization results, it has been observed that the calculated RAWR tends to follow trends similar to that of the hardness. As shown in Fig. 3, there is correlation between hardness and RAWR for both the APS and D-gun spray processes. This shows a trend that the higher hardness coating resulted in the best abrasive wear resistance.

**3.5.2 Sliding Wear Test Results.** The wear rates of all the coated pins, determined as the volume loss of the coated pin in cubic millimeters per meter of sliding distance, are presented in Tables 9 and 10. As indicated in Table 12, primary gas flow alone had a significant effect in lowering the wear rate and had

**Table 12 Contribution ratios and optimized levels for plasma spray process parameters**

Desired coating attribute	Processing factors ( $\rho\%$ /level)			
	Primary gas flow	Plasma arc current	Powder feed rate	Spray distance
Low roughness	3.59/+1	12.51/+1	0.04/-1	71.63/+1
High hardness	8.73/+1	4.82/+1	0.20/-1	82.00/-1
Low porosity	7.10/+1	23.47/+1	5.08/-1	54.36/-1
High RAWR	16.96/+1	1.03/+1	2.70/-1	59.12/-1
Low wear rate	25.30/+1	4.95/+1	4.80/+1	6.40/-1

a contribution ratio of 25.3%; other parameters had only small contribution ratios. Similarly, frequency of detonations had a major contribution ratio of 55.9%, affecting the sliding wear rate in the D-gun process (Table 13). The variation in the wear rates for all the coatings indicates that all the APS coatings exhibit a slightly higher wear rate than the corresponding D-gun coatings.

### 3.6 Optimizing APS and D-Gun Spray Process Parameters

Selection of optimum levels of the designed factors can produce consistently good-quality thermal spray coatings. In the Taguchi method, usually there are three categories of the quality characteristic in the ANOVA; *i.e.*, “higher the better,” “lower the better,” and “nominally the best.” The optimal parameters are selected based on the required coating quality. For hardness and RWAR, “higher the better” criteria were chosen and, therefore, the highest values are circled, indicating the parametric level that should yield the highest hardness, whereas for surface roughness, porosity, and wear rate, “lower the better” criteria were chosen.<sup>[10,11]</sup> The preferred levels of the APS and D-gun process parameters obtained from the effects of analysis are listed in Tables 12 and 13 for the desired coating attributes. For all of the coating properties studied (except roughness), spray distance was the single most influential parameter, with lower distance being the optimum for the APS process. The remaining variables shifted in importance depending on the property examined. Further, from the tables, it is quite understandable that the variables corresponding to high hardness, low porosity, and high RAWR were located at the same parameter levels for the APS process. The present investigation shows that Al<sub>2</sub>O<sub>3</sub> coatings of low porosity, high hardness, and high RAWR could be obtained by using the following APS process parameters: primary gas flow of 78 L/min, arc current of 500 A, powder feed rate of 20 g/min, and spray distance of 60 mm.

In the case of D-gun, spray distance and fuel ratio were the dominating factors, with lower distance and higher fuel ratio being optimum for all of the properties studied. The Al<sub>2</sub>O<sub>3</sub> coatings with extremely good wear characteristics could be obtained by using the following D-gun process parameters: fuel ratio of 1:2.8, detonation frequency of 2 Hz, and spray distance of 180 mm. The remaining variable, carrier gas flow rate, could be shifted in importance depending on the property examined, similar to that of the APS process.

**Table 13 Contribution ratios and optimized levels for D-gun spray process parameters**

Desired coating attribute	Processing factors ( $\rho\%$ /level)			
	Fuel ratio (C <sub>2</sub> H <sub>2</sub> /O <sub>2</sub> )	Carrier gas flow rate	Frequency of detonations	Spray distance
Low roughness	9.75/+1	0.32/-1	0.09/-1	84.12/+1
High hardness	30.43/+1	3.47/-1	2.47/-1	45.90/-1
Low porosity	49.58/+1	0.33/-1	0.27/-1	43.76/-1
High RAWR	29.74/+1	1.30/+1	3.75/-1	45.90/-1
Low wear rate	6.69/+1	2.68/-1	55.92/-1	5.87/-1

## 4. Conclusions

Taguchi style fractional-factorial (L<sub>8</sub>) experiments were used to study and optimize both plasma and D-gun processes for alumina coatings. Major parameters investigated in the studies included primary gas flow, arc current, powder feed rate, and spray distance for the plasma spraying and fuel ratio, carrier gas flow rate, frequency of detonations, and spray distance for the D-gun spraying. Coating attributes evaluated included surface roughness, microhardness, porosity, abrasion, and sliding wear. According to the results, samples PA02 and DA03 were the best Al<sub>2</sub>O<sub>3</sub> coatings formed by plasma and D-gun spraying, respectively. Based on the coating characterization results, the following conclusions may be drawn.

- D-gun-sprayed coatings consistently exhibit denser microstructure and higher hardness than the corresponding APS coatings. Presumably, as a consequence of the above, the D-gun-sprayed coatings are also found to outperform the corresponding APS coatings under all the wear modes studied.
- In the Taguchi statistical evaluation, spray distance, primary gas flow, and arc current were identified as the major controlling factors in the APS process, whereas spray distance and fuel ratio were the significant factors in the D-gun process for the measured responses.
- For the APS process, higher primary gas flow, higher arc current, and shorter spray distance are necessary for higher hardness, lower porosity, and higher abrasive wear resistant coatings, whereas for the D-gun process, higher fuel ratio and shorter spray distance are necessary.
- In view of both cases, it has been observed that the highest as-sprayed coating hardness had the highest RAWR and this shows a trend that the higher hardness coating resulted in the best abrasive wear resistance.
- In controlling the sliding wear, primary gas flow and frequency of detonations were the dominant factors for the APS and D-gun spray processes, respectively. Other factors have only small contribution ratios.
- The present investigation shows that the quality of alumina coatings is directly related to the corresponding coating microstructure, which is significantly influenced by the spray parameters employed. Though it is evident that the D-gun-sprayed coatings consistently exhibit denser microstructure, higher hardness values, and superior tribological perfor-

mance, the performance of plasma-sprayed coatings can be improved further by employing the Taguchi analysis.

- In conclusion, the Taguchi evaluation employed in the present study led to optimized process variables for the best wear resistant alumina coatings.

### Acknowledgments

The authors are grateful to D. Sen, K.R.C. Somaraju, D. Jayaram, and V.S.R.A. Sarma for their help in generating the coated specimens. The authors (PS) and (VS) thank the Director of ARC-I, Hyderabad, and the Director of DMRL, Hyderabad, for giving permission to carry out the present study. Also one of the authors (PS) acknowledges the award of Senior Research Fellowship (SRF) by the Council of Scientific and Industrial Research (CSIR), Government of India.

### References

1. G. Barbezat, A.R. Nicoll, and A. Sickinger: *Wear*, 1993, vol. 162–164, pp. 529–37.
2. K. Ebert, C. Verpoort, and C. Karsten: *Mater. Sci. Forum*, 1994, vol. 163–165, pp. 587–94.
3. K. Niemi, P. Vuoristo, E. Kumpulainen, P. Sorsa, and T. Mantyla: *Recent Developments in the Characteristics of Thermally Sprayed Oxide Coatings, Thermal Spraying Current Status and Future Trends*, High Temperature Society of Japan, Welding Research Institute, Osaka University, Osaka, Japan, 1995, pp. 687–92.
4. A.S. Khanna and A.K. Pattanaik: *Trans. Metal Finishers' Assoc. India*, 1997, vol. 6, pp. 187–205.
5. G. Sundararajan, K.R.C. Somaraju, and D. Srinivasa Rao: in *Surface Modification Technologies X*, T.S. Sudarshan, K.A. Khor, and M. Jeandin, eds., The Institute of Materials, London, 1997, pp. 367–84.
6. K. Niemi, P. Vuoristo, and T. Mantyla: *J. Thermal Spray Technol.*, 1994, vol. 3, pp. 199–203.
7. C.J.S. Guest: *Trans. IMF*, 1986, vol. 64, pp. 33–38.
8. Y. Wang: *Wear*, 1993, vol. 161, pp. 69–78.
9. W.L. Riggs, R.K. Betz, and N. Jayaraman: in *Thermal Spray Research and Applications*, T.F. Bernecki, ed., ASM International, Materials Park, OH, 1990, pp. 711–28.
10. T. Chon, A. Aly, B. Kushner, A. Rotolico, and W.L. Riggs: in *Thermal Spray Research and Applications*, T.F. Bernecki, ed., ASM International, Materials Park, OH, 1990, pp. 681–93.
11. J.E. Nerz, B.A. Kushner, and A.J. Rotolico: in *Thermal Spray Coatings: Research, Design and Applications*, C.C. Berndt and T.F. Bernecki, eds., ASM International, Materials Park, OH, 1993, pp. 669–73.
12. M. Lynn, S. Lynn, D.J. Varacalle, and W.L. Riggs II: in *Thermal Spray Coatings: Research, Design and Applications*, C.C. Berndt and T.F. Bernecki, eds., ASM International, Materials Park, OH, 1993, pp. 315–22.
13. G. Taguchi, and S. Konishi: *Taguchi Methods: Orthogonal Arrays and Linear Graphs*, ASI Press, 1987.
14. G.E.P. Box and W.G. Hunter: *Statistics for Experimenters*, John Wiley & Sons Inc., New York, NY, 1978.
15. N.L. Frigon and D. Mathews: *Practical Guide to Experimental Design*, John Wiley & Sons, Inc., New York, NY, 1997.
16. G. Sundararajan, K.U.M. Prasad, D.S. Rao, and S.V. Joshi: *J. Mater. Eng. Perform.*, 1998, vol. 7, pp. 343–51.
17. V. Kadyrov, Y. Margarita, D. Sen, D. Srinivasa Rao, K.P. Rao, and A.V. Saibaba: in *Transactions of the Powder Metallurgy Association of India*, P. Ramakrishnan, ed., 1993, vol. 20, pp. 1–5.
18. Standard Practice for Conducting Dry Sand/Rubber Wheel Abrasion Tests, ASTM G65–85, ASTM, Philadelphia, PA, 1985.
19. G. Sundararajan, D. Srinivasa Rao, D. Sen, and K.R.C. Somaraju: in *Surface Modification Technologies X*, T.S. Sudarshan, M. Jeandin, and K.A. Khor, eds., The Institute of Materials, London, 1998, pp. 872–86.
20. Metco Technical Bulletin for Al<sub>2</sub>O<sub>3</sub> Powder, Metco, Sept. 1979.
21. A. Vardelle, M. Vardelle, and P. Fauchais: *Plasma Chem. Plasma Processing*, 1982, vol. 2, pp. 255–91.
22. R.G. Smith: in *Science and Technology of Surface Coatings*, B.N. Chapman, ed., Academic Press, London, 1974, pp. 271–97.
23. Y.A. Kharlamov: *Mater. Sci. Eng.*, 1986, vol. 93, pp. 1–37.
24. Y.A. Kharlamov: *Thin Solid Films*, 1978, vol. 54, pp. 271–78.